Artificial Intelligence in Geosciences 3 (2022) 8–13

Contents lists available at ScienceDirect

Artificial Intelligence in Geosciences

journal homepage: www.keaipublishing.com/en/journals/artificial-intelligence-in-geosciences

A convolutional recurrent neural network for strong convective rainfall nowcasting using weather radar data in Southeastern Brazil

Angelica N. Caseri [a,*], Leonardo Bacelar Lima Santos [a], Stephan Stephany [b]

[a] CEMADEN - Estrada Dr. Altino Bondensan, 500 - Eug^enio de Melo, S.J.Campos, Brazil
[b] INPE - Av. dos Astronautas, 1758 - Jardim da Granja, S. J. Campos, 12.227-001, Brazil

ARTICLE INFO

Keywords:
Nowcasting
Rainfall
Extreme events
Weather radar
Deep learning

ABSTRACT

Strong convective systems and the associated heavy rainfall events can trig-ger floods and landslides with severe detrimental consequences. These events have a high spatio-temporal variability, being difficult to predict by standard meteorological numerical models. This work proposes the M5Images method for performing the very short-term prediction (nowcasting) of heavy convective rainfall using weather radar data by means of a convolutional recurrent neural network. The recurrent part of it is a Long Short-Term Memory (LSTM) neural network. Prediction tests were performed for the city and surroundings of Campinas, located in the Southeastern Brazil. The convolutional recurrent neural network was trained using time series of rainfall rate images derived from weather radar data for a selected set of heavy rainfall events. The attained pre-diction performance was better than that given by the persistence forecasting method for different prediction times.

1. Introduction

The rainfall associated with strong convective systems usually triggers floods and landslides that hit countless parts of the world every year, causing substantial socioeconomic damages. According to (Kron, 2003), 50% of the damage caused by natural disasters is due to flash floods, which are bound to a limited area, and present a fast dynamic (Cristiano et al., 2017). Flash floods are usually due to high rainfall associated with strong convective events (Li et al., 2022). Therefore, heavy rainfall predictions may feed flood forecasting systems able to issue early warnings to affected areas ((Caseri et al., 2016), (Santos et al., 2017)). In particular, such warnings are more relevant for tropical countries like Brazil, which frequently present strong convective rainfall events. Heavy rainfall event can be defined by 24-h accumulated rainfall more than 64.5 mm as heavy rainfall, very heavy rainfall as more than 124.5 mm, and extremely heavy rainfall as more than 244.5 mm (Pune, 2017).

In the last years, artificial intelligence methods have been increasingly used to complement numerical models in the prediction of complex phenomena (Schmidhuber, 2015). Such methods are typically based on a machine learning algorithm, which is ad-justed/trained using known observational data of a given phenomenon in order to detect it from new data. One of the most commonly employed algorithms are neural networks. As an example in Meteorology (Aoki, 2017), used a Convolutional Neural Network (CNN) (Springenberg et al., 2014),) method for rainfall detection and estimation using satellite images (NOAA GOES Imagery). Other examples, more related to this work, are (Shi et al., 2015) and (Heye et al., 2017) that applied a Long Short-term Memory (LSTM) recurrent neural network for rainfall forecasts using weather radar data. Additional approaches using NASA Global Precipitation Measurement (GPM) satellite data include a model based on a convolutional LSTM to predict short-term precipitation events (Kumar et al., 2020), and a CNN-LSTM neural network for rainfall nowcasting (Gamboa-Villafruela et al., 2021). Other CNN-LSTM models were developed to make flow predictions in order to simulate hydrological rainfall-runoff models, like (Deng et al., 2022) or (Li et al., 2022), using two dimensional rainfall radar maps, and tested for German watersheds.

This work proposes the very nowcasting of heavy rainfall events by mean of a deep learning approach, a machine learning algorithm using weather radar data. According to the World Meteorological Organization[1], nowcasting refers to up to 6 h forecast. These rainfall events have a high spatio-temporal variability, being difficult to predict by standard numerical models. Weather radars allow the real-time monitoring of convective rainfall, thus providing time series of images that can be employed by the machine learning algorithm, in this case, a convolutional recurrent neural network.

In this study, a new method called M5Images is proposed for heavy

* Corresponding author.
E-mail addresses: angelica.caseri@gmail.com (A.N. Caseri), santoslbl@gmail.com (L.B. Lima Santos), stephan.stephany@inpe.br (S. Stephany).

https://doi.org/10.1016/j.aiig.2022.06.001
Received 6 April 2022; Received in revised form 31 May 2022; Accepted 2 June 2022
Available online 13 June 2022

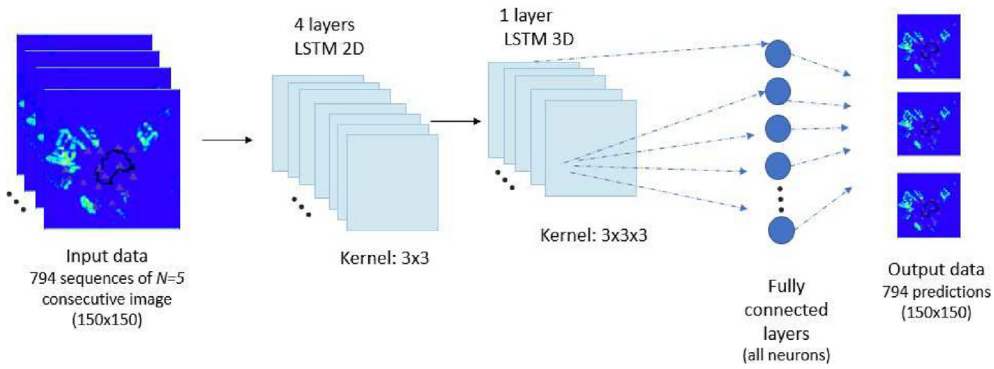

Fig. 1. Illustration of the proposed CNN-LSTM neural network architecture during the training phase (along the training, 794 sequences with N = 5 images are inputted, and 794 images are outputted).

rainfall nowcasting, using weather radar data as input data for a convolutional recurrent neural network. The recurrent part of it is a Long Short-Term Memory (LSTM) neural network. The area of study is the city of Campinas, in the Southeastern Brazil, and its surrounding areas. Weather radar data was processed to yield a time series of 2D images of precipitation rate. M5Images is a predictive algorithm intended to predict rainfall rate values above a defined threshold for the pixels of the considered grid. The use of a rainfall rate threshold was suggested by (Mason and Graham, 1999), and adopted here with a value of 5 mm/h, similarly as in (Caseri et al., 2020). The proposed approach differs from previous ones by using only data of heavy and very heavy rainfall events in the training phase of the neural network, besides proposing a new correction factor to improve the predictions.

The attained prediction performance of the M5Images method for the considered test cases was better than that given by the persistence forecasting method (PFM), taken as a reference method, for different prediction advance times. The PFM simply considers the last observation as a forecast for the next observation. This article presents the following sections: Section 2 describes the methodology including the proposed neural network, data partitioning and validation scheme, and the number of input sequence of images in the training/validation and test phases. Section 3 is about the about the location, radar data and rainfall rate images. Section 4 shows the prediction results, and the prediction performance analyzed and discussed using standard metrics. Finally, Section 5 contains conclusions and final remarks, as well as suggestions for future works.

2. The proposed convolutional recurrent neural network

The neural network used here derives from the CNN-LSTM of (Hochreiter & Schmidhuber, 1997), proposed to solve the problem of vanishing gradient, a particular problem with recurrent neural networks. In the training phase, network weights are iteratively updated using an error gradient in order to correct the network output. However, the calculation of such gradient may yield zero due to the large number of time steps of a temporal sequence. The LSTM neural network is a type of recurrent neural network with the ability dealing better with the vanishing gradient problem and thus being suitable for prediction problems involving time series. LSTM networks are based on a cell with an entrance gate, an output gate, and a forgetting gate, which regulate the flow of information in and out of the cell, in a way that some neuron values are preserved at arbitrary time intervals (Sherstinsky, 2018).

The historical meteorological series of 2D precipitation rate maps is seen as a data cube, where the third dimension is time. The 3D CNN-LSTM neural network was only trained with time series of images related to a set of heavy and very heavy rainfall events, thus learning the characteristic patterns of such events, including their evolution trends. This CNN-LSTM neural network is of the kind many-to-one, i.e. an input sequence with any number of rainfall images sorted in time is used to output a single image. Here, an image is given by a finite set of grid points covering the area of study, with a rainfall rate in mm/h at each one.

In this work, the size of the input sequence of images used in the training and test phases are denoted by TSI and PSI, respectively. Different values of TSI and PSI were evaluated, resulting in the adoption of a 5:1 ratio for the training/validation phase (TSI equal to 5), which means that a sequence of 5 images feeds the neural network to predict the 6th next image. For the test phase, 3:1 and 2:1 ratios were adopted (PSI equal to 2 or 3), corresponding to a sequence of 2 or 3 images feeding the neural network to predict the 3rd or 4th next images, respectively. These values for TSI and PSI resulted in a better prediction performance, as shown in Section 4.

Fig. 1 presents the proposed neural network architecture, which includes four 2D–CNN–LSTM layers and a single 3D–CNN–LSTM layer. Images have 150 × 150 pixels or grid points. In the training phase, each sequence of 5 images (ordered in time) traverse successively the four 2D–CNN–LSTM (each one applying a 3 × 3 kernel to the image) and the resulting 5-image set is then merged into a 5 × 150 × 150 array in the 3D–CNN–LSTM layer that uses a 3 × 3 × 3 kernel. Finally, each of these arrays is fed to a fully connected layer rendering a 150 × 150 output image. The only difference in the test phase is the input, given by 2-image or 3-image sequences.

After each layer, a normalization is performed. The same padding scheme was applied to all layers, thus preserving the spatial dimension of the input data. The activation function is one particular non-linear sigmoid (S-shaped) function, the logistic function, which allows nodes to learn complex structures (Chandra, 2003). As in most neural networks, the training involves the updating of the set of weight matrices in order to minimize the loss function, that evaluates the difference between predicted and observed precipitation rates. Here, the loss function is given by the Mean Square Error (MSE) metric. In the training of a neural network, an epoch is defined as the number of times that the training is performed using all the instances/samples of the training set. The training set is split in to equal-size batches, and for each batch, the weights and bias of the network are adjusted as a function of the loss function, using a backpropagation scheme. It is expected that along the epochs, the neural network converge, minimizing the loss function. Here, each sample/instance is composed of the sequence of 5 consecutive images, each one with the rainfall rates of all pixels. In order to find an optimal number of epochs, some tests were performed for 10, 30, 50, and even more than 50 epochs in the training phase. The prediction error decreased from 10 to 30 epochs, but there was no significant change above 30 epochs, and therefore, the adopted number of epochs was 30.

The proposed CNN-LSTM model is trained and validated with data of a selected set of heavy and very heavy rainfall events in the chosen area of study. Temporal resolution of the time series of images is 10 min, but the training employs 5-image sequences (TSI equal to 5) extracted from the time series with N images of a given event using a sliding window of size W = 5 that advances one image (10 min) each step, thus rendering a

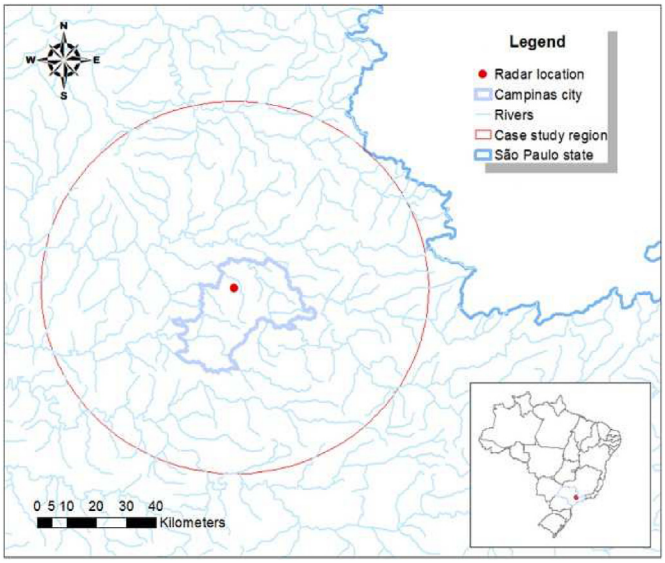

Fig. 2. Area of study (city of Campinas and surroundings) and the location of the X-band weather radar (red dot).

total of (N–W+1) sequences for each event of the training set. These sequences allow the CNN-LSTM network to assimilate the temporal evolution of the rainfall events.

In addition, a correction scheme for the rainfall forecasts is also proposed in order to deal with the rainfall forecast underestimation observed in the tests, providing more reliable forecasts. The scheme employs a multiplicative correction factor derived from the fist observed image, as follows. Considering predictions for 10, 20 and 30 min, the mean absolute percentage error (MAPE) is calculated for all pixels between observation and the first prediction (10 min). The MAPE is then used to derive the correction factor to be applied for the further 20 and 30 min predictions, being applied to all the pixels. This study was performed using the R language with the following packages: keras, tensorflow, raster, Metrics, MLmetrics.

Evaluation of the prediction/forecast performance was done by the metric Area Under the Curve (AUC) of the ROC (Receiver Operating Characteristic) curve2, and also the Root Mean Square Error (RMSE). The RMSE is calculated using the rainfall rate continuous values of the pixels of the predicted and of the observed images. However, the ROC AUC metric is defined for a binary classifier/predictor, not for continuous values as in this case. This issue was solved by assigning a pixel as being rainfall occurrence if it presents a rainfall rate above the defined threshold of 5 mm/h or the opposite if below the threshold, thus defining two classes: occurrence or not of rainfall. The ROC curve is a x-y plot that shows the balance between true positives (y values) and the false positives (x) for a binary classifier, with the linear curve with 45° slope corresponding to a random classifier. The ROC AUC ranges between 0 and 1, with the latter value expressing a perfect classifier, and a value of 0.5 corresponding to a random classifier.

3. Case study location and data

The proposed approach was applied to the city and surroundings of Campinas (Brazil) using data of 2016 and 2017, mostly in summertime. The choice of this location was due to the record of numerous flood events in recent years. The weather radar is a mobile X-band radar, that provided full coverage of the area of study, as shown in Fig. 2. It has dual-polarization (vertical and horizontal) and electronic beam opening capability, providing a complete volume scan every 10 min. Radar spatial resolution corresponds to 200 m^2 in the horizontal plane, but was reduced to a 1 km × 1 km resolution yielding images with 150 × 150 pixels. The use of dual-polarization weather radars is recent in Brazil, contributing to improve the associated research in Meteorology (Seron et al., 2019).

Table 1
Characteristics of the selected rainfall events.

Event ID	Starting date and time	Duration (h)	Maximum observed total rainfall (mm)	Phase
1	2016/11/23 06:30	20	169	Training
2	2016/11/26 15:30	8	149	Training
3	2016/11/27 13:30	15	150	Training
4	2016/11/28 15:30	17	183	Test
5	2016/12/03 14:30	9	117	Test
6	2017/02/18 00:30	5	113	Test
7	2017/02/24 15:30	11	172	Training
8	2017/02/25 10:30	13	83	Training
9	2017/02/26 13:30	11	144	Training
10	2017/03/02 11:00	20	168	Training
11	2017/05/19 02:00	17	191	Training
12	2017/05/21 12:30	18	139	Training

Campinas is located in a transition zone, during the summer, precipitation is mostly convective and modulated by the presence of the Southern Atlantic Convergence Zone (SACZ). Campinas has more than 1 million inhabitants and shows impressive urban growth. Its demographic growth, like most Brazilian cities, has occurred in a chaotic way with a lack of organization and infrastructure. This disorderly growth contributes to the increase in the frequency and magnitude of floods and extreme events causing socio-economic damage in the region (Vicente et al., 2004).

A selection of heavy and very heavy rainfall events in the area of study was made using the historical series of images with 10 min resolution obtained by the mobile X-band weather radar installed in Campinas. Radar reflectivity values (Z, in mm6/m3) were mapped to rainfall rates (R, in mm/h) using a suitable Z-R relation (Marshall-Palmer). The rainfall rate threshold of 5 mm/h was adopted for the selection of the rainfall events, in order to filter out events with low rainfall rates.

Table 1 shows, for each selected rainfall event, the starting date and time, duration in hours, and maximum observed rainfall rate summing up all pixels, and considering all time steps of the event. In this table, the 12 heavy and very heavy rainfall events were selected using the threshold of 5 mm/h. All these events lasted less than 24 h and presented rainfall amounts between 83 and 191 mm. Considering the Southeast of Brazil, one single event may represent the amount of rainfall of an entire month. These totals are shown to illustrate the severity of these rainfall events, but were not employed in the prediction tests.

These twelve events were divided into training and test sets, with 9 and 3 events, respectively. Considering the training events, 95% of the images were taken for training and the remaining 5% for validation. The validation phase is intended to optimize the neural network hyperparameters, in this case, the loss function (given by the MSE), batch size and number of epochs. The training/validation set includes a total of 133 h or 798 images sampled with 10 min resolution, resulting by the sliding window scheme in (794–5+1) or 794 sequences of 5 consecutive images (TSI equal to 5). The test set comprehends 31 h or 186 images sampled with 10 min resolution, resulting in (186–5+1) or 182 sequences of 5 consecutive images (TSI equal to 5).

Table 2
AUC ROC results (threshold 5 mm/h) for different combinations of TSI and PSI (number of input images for training and test, respectively), and for different prediction times.

TSI	PSI	10 min	20 min	30 min	40 min	50 min
5 images	2 images	0.90	0.62	0.56		
	3 images	0.87	0.67			
6 images	2 images	0.50	0.60	0.50	0.50	
	3 images	0.50	0.51	0.50		
	4 images	0.52	0.61			
7 images	2 images	0.53	0.53	0.46		
	3 images	0.54	0.47	0.51	0.52	0.50
	4 images	0.46	0.51	0.50	0.50	
	5images	0.52	0.50			

Table 3
RMSE results for different combinations of TSI and PSI (number of input images for training and test, respectively), and for different prediction times.

TSI	PSI	10 min	20 min	30 min	40 min	50 min
5 images	2 images	1.00	2.64	2.64		
	3 images	0.89	3.01			
6 images	2 images	1.30	0.25	3.1	0.11	
	3 images	2.92	12.99	2.95		
	4 images	6.8	2.98			
7 images	2 images	4.63	9.63	11.83	10.10	7.00
	3 images	5.61	6.77	6.20	4.67	
	4 images	6.70	6.13	4.64		
	5images	6.28	4.17			

4. Rainfall forecast results

The CNN-LSTM neural network was trained, validated and tested using the radar data described in the preceding section. As mentioned, after the training phase, the validation phase allowed to optimize the network hyperparameters, and the network was then used for the test phase. In addition, experimentation allowed to optimize the size of the sequence of images used in the training phase (TSI), as well as the size of the sequence of images used for prediction in the test phase (PSI).

Performance evaluation of the prediction was performed for TSI range of 5–7 and PSI range of 2–5, as shown in Table 2 and 3 for the ROC AUC and the RMSE, respectively, both considering a threshold of 5 mm/h. The best combination was TSI/PSI of 5/3 (only slightly better than 5/2) considering ROC AUC, and thus was adopted henceforth in this work.

As mentioned above, in the training and validation phases, consecutive sequences of 5 images (TSI equal to 5) were also employed to predict the 6th next one with a 5:1 ratio, but in the test phase, a 2:1 ratio (PSI equal to 2) was used for the 3rd image (10-min prediction), and adding the just predicted grid, a 3:1 (PSI equal to 3) ratio was then used for the 4th and 5th images (20-min and 30-min predictions, respectively).

These predictions correspond to the rainfall rate images with anticipation of 10, 20 and 30 min. Fig. 3 presents a flowchart summarizing the main steps and methods of the proposed approach.

Fig. 4 shows the rainfall forecasts generated by the M5Images method for prediction times of 10, 20 and 30 min, compared to the observed data, for a particular instant of time (2016/11/28 20:10 h), considering the area of study. It shows that the prediction performance worsen with the increase of prediction time. Although the 10-min prediction is very similar to the observed rainfall, the predictions for 20-min and 30-min were not able to identify the rainfall zone and rainfall intensity for the corresponding pixels. The high variability of these rainfall events and their low spatio-temporal correlation render the prediction difficult for higher prediction times (Caseri et al., 2020).

As already mentioned, the evaluation of the prediction/forecast performance was done by two standard metrics, the Area Under the Curve (AUC) of the ROC (Receiver Operating Characteristic) curve, and also the Root Mean Square Error (RMSE) comparing the pixels of the predicted and of the observed images. RMSE is calculated employing the continuous rainfall rate values of the pixels, while ROC AUC required a kind of binarization based on the adopted threshold of 5 mm/h. A value of rainfall rate above the threshold is mapped as a rainfall occurrence, whereas a value below, as not.

These metrics were calculated for each sequence of 3 predicted consecutive images, taking into account all the pixels of these images. The same metrics were applied for the PFM, which considers the last image as the forecast for the next grid, pixel to pixel. Therefore, such method was adopted as a reference for the proposed approach.

Fig. 5 shows the AUC of the forecasts produced by the M5images and the PFM methods, considering three prediction times (10, 20 and 30 min), and a threshold of 5 mm/h of rainfall. For both methods, the prediction performance decreases as the prediction time increases, but the M5Images method performed better, even for a 30-min prediction time. Considering the shortest 10- minute forecast, the M5Images AUC ROC was close to 1, while the PFM one was close to 0.7.

Finally, as shown in Fig. 6, the RMSE mean values of the M5Images forecasts were 2.0, 3.3 and 3.6 mm/h, respectively, for 10, 20 and 30 min prediction times, while the corresponding RMSE mean values of the PFM forecasts were 4.0, 4.5 and 4.7 mm/h. As expected, the higher the prediction time, the lower is the prediction performance.

5. Conclusion

Rainfall nowcasting is essential for early warning systems, especially in regions characterized by heavy rainfall events. This work presents the M5Images method that employs a Machine Learning approach, a CNN-LSTM convolutional recurrent neural network for the prediction of rainfall rate images using temporal series of rainfall rates derived from

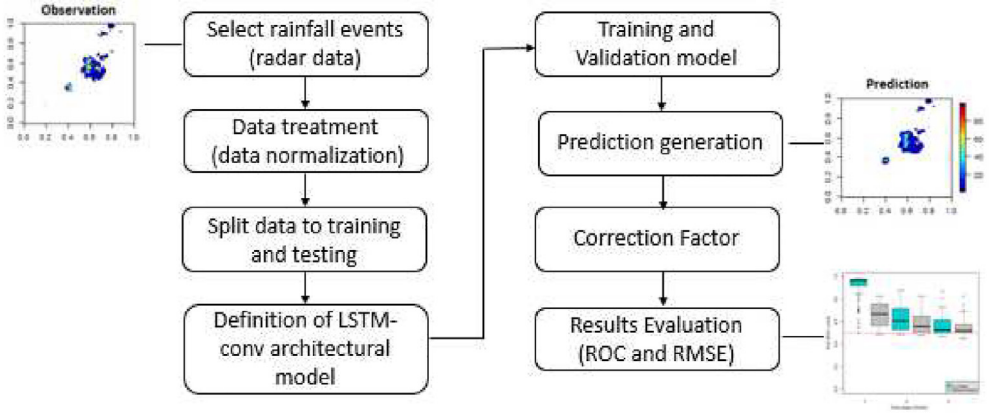

Fig. 3. Flowchart of the stages of the proposed M5Images method.

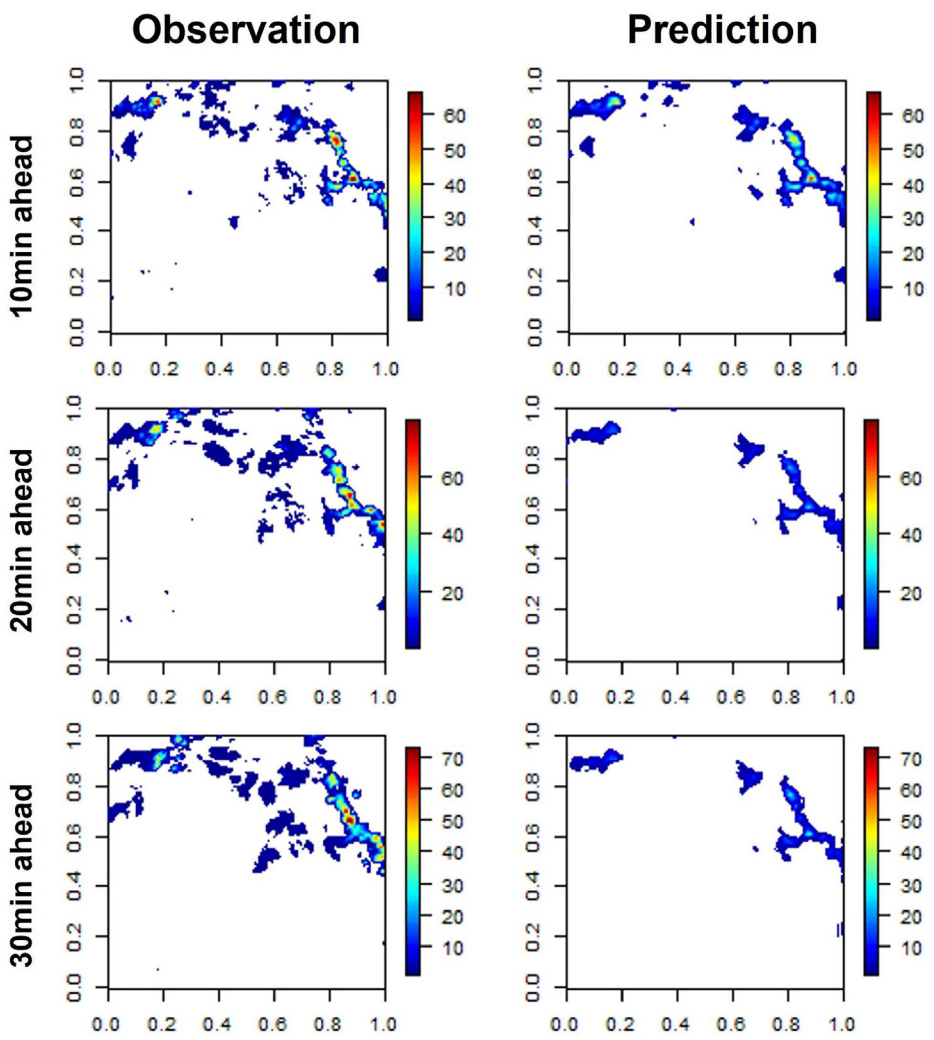

Fig. 4. Observed and M5Images-generated forecast rainfall rate images for the three pre-diction times of 10, 20 and 30 min.

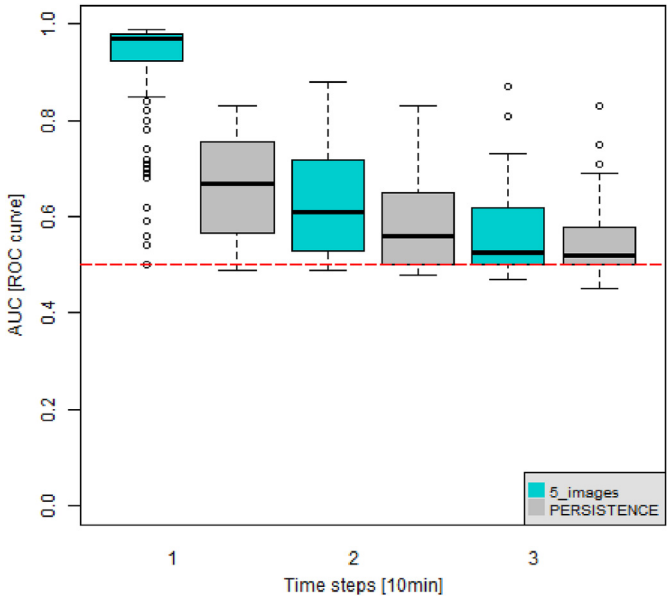

Fig. 5. Box plot of the AUC of the forecasts made by the M5Images (blue) and Persistence (light gray) methods for (left to right) 10, 20 and 30 min of prediction time.

weather radar data. An innovative aspect is the training phase of the network, which is performed using only images corresponding to heavy and very heavy rainfall events in the considered area of study.

Tests were performed for prediction times of 10, 20 and 30 min for the area of study, the Brazilian city of Campinas and its surroundings. As expected, the higher the prediction time, the lesser the prediction accuracy, since ensuing predictions employ the former ones. These rainfall rate forecasts made by the M5Images method were compared to the corresponding rainfall rates derived from weather radar data, and also to the forecasts given by the Persistence method. All forecasts were evaluated by the ROC-AUC and RMSE metrics, showing the better prediction performance of the M5Images forecasts. Considering time series of images with 10-min resolution, the CNN-LSTM network of the M5Images method is trained using input sequences of 5 consecutive im-ages (TSI equal to 5), and perform predictions using input sequences of 2 or 3 consecutive images (PSI equal to 2 or 3) to predict the next images using a sliding window of consecutive images (10–30 min). Optimal values of TSI and PSI, as well the number of epochs of the training phase (30) were defined by experimentation.

It is foreseen to employ GPU processing, since the training phase demands 3–4 days on a standard PC, and there are specific machine learning libraries for GPU use. Future work also includes the implementation of ensemble schemes that consists of generating not one, but several forecasts using the same input data for a finite set of different predictors. The ensemble yields a finite set of forecast images, being the

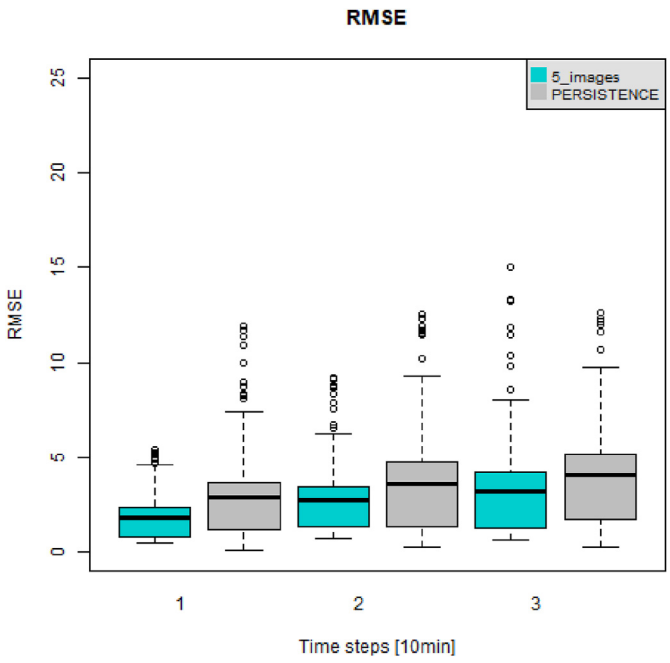

Fig. 6. Box plot of the RMSE of the forecasts made by the M5Images (blue) and Persistence (light gray) methods for (left to right) 10, 20 and 30 min of prediction time.

resulting forecast given by averaging pixel-to-pixel these images. As an example, a set of different predictors can be obtained using a drop-out technique that randomly erases one of the fully-connected output layers that render the network output. Another ensembles can result from using different network architecture or different weight initialization scheme for each predictor. In addition, the prediction performance of the M5Images method performance will be evaluated for prediction times longer than 30 min, since for nowcasting, the higher the prediction time, the better the usefulness for early warning systems.

Declaration of competing interest

The authors declare that they have no known competing financial interests or personal relationships that could have appeared to influence the work reported in this paper.

Acknowledgment

The authors thank the Fundação de Amparo à Pesquisa do Estado de São Paulo (FAPESP) Grant Numbers 2015/50122–0, 17/00275–0 and 15/14497–0; Conselho Nacional de Desenvolvimento Científico e Tecnológico (CNPq) Grant Number 420338/2018- 7 and DFG-IRTG Grant Number 1740/2 for the financial and research supports.

This study was financed in part by the Coordenação de Aperfeiçoamento de Pessoal de Nível Superior - Brasil (CAPES) - Finance Code 001.

References

Aoki, P.M., 2017. CNNs for precipitation estimation from geostationary satellite imagery. CS 231N Project Rep. 9.

Caseri, N.A., Angelis, C.F, Sperling, V.B., Leblois, E., 2020. Statistical Variability of Severe Rainfall in Southeastern Brazil. Anuario IGEO.

Caseri, A., Javelle, P., Ramos, M.H., Leblois, E., 2016. Generating precipitation ensembles for flood alert and risk management. J. Flood Risk Manag. 9 (4), 402–415. https://doi.org/10.1111/jfr3.12203.

Chandra, P., 2003. Sigmoidal function classes for feedforward artificial neural net- works. Neural Process. Lett. 18.

Cristiano, E., Veldhuis, M.-C. t., Giesen, N.v. d., 2017. Spatial and temporal variability of rainfall and their effects on hydrological response in urban areas – a review. Hydrol. Earth Syst. Sci. 21 (7), 3859–3878. https://doi.org/10.5194/hess-21-3859-2017.

Gamboa-Villafruela, C.J., Fernández-Alvarez, J.C., Márquez-Mijares, M., Pérez-Alarcón, A., Batista-Leyva, A.J., 2021. Convolutional lstm architecture for precipitation nowcasting using satellite data. Environ. Sci. Proc. 8 (1).

Heye, A., Venkatesan, K., Cain, J., 2017. Precipitation nowcasting: leveraging deep recurrent convolutional neural networks. In: Proceedings of the Cray User Group (CUG) 2017, p. 8.

Hochreiter, S., Schmidhuber, J., 1997. Long short-term memory. Neural Comput. 9 (8), 1735–1780. https://doi.org/10.1162/neco.1997.9.8.1735.

Kron, W., 2003. Flood catastrophes: causes-losses-prevention from an interna- tional re-insures's viewpoint. In: Proceedings. Science Press.

Kumar, A., Islam, T., Sekimoto, Y., Mattmann, C., Wilson, B., 2020. Convcast: an embedded convolutional lstm based architecture for precipitation now- casting using satellite data. PLoS One 15, 1–18. https://doi.org/10.1371/journal.pone.0230114.

Li, P., Zhang, J., Krebs, P., 2022. Prediction of flow based on a cnn-lstm combined deep learning approach. Water 14 (6).

Mason, S.J., Graham, N.E., 1999. Conditional probabilities, relative operat- ing characteristics, and relative operating levels. Weather Forecast. 14 (5), 713–725. https://doi.org/10.1175/1520-0434(1999)014<0713:CPROCA>2.0.CO;2.

Pune, I., 2017. Met Glossary. https://www.imdpune.gov.in/Weather/Reports/glossary.pdf.

Santos, L., Carvalho, T., Anderson, L.O., Rudorff, C., Marchezini, V., Londe, L.R., Saito, S.M., 2017. An rs-gis-based comprehensive impact assessment of floods-a case study in Madeira river, Western Brazilian Amazon. Geosci. Rem. Sens. Lett. IEEE 1–4.

Schmidhuber, J., 2015. Deep learning in neural networks: an overview. Neural Network. 61, 85–117. https://doi.org/10.1016/j.neunet.2014.09.003.

Seron, W., Santos, L.B.L., Dolif Neto, G., Quiles, M., Candido, O.A., 2019. Com- munity detection in very-high resolution meteorological networks. Geosci. Rem. Sens. Lett. IEEE 1, 1–4.

Sherstinsky, A., 2018. Fundamentals of recurrent neural network (RNN) and long short-term memory (LSTM) network. Phys. Nonlinear Phenom. https://doi.org/10.1016/j.physd.2019.132306.

Shi, X., Chen, Z., Wang, H., Yeung, D.-Y., Wong, W.-k., Woo, W.-c., 2015. Con- volutional LSTM network: a machine learning approach for precipitation nowcasting. In: Proceedings of the 28th International Conference on Neural Information Processing Systems arXiv:1506.04214.

Springenberg, J.T., Dosovitskiy, A., Brox, T., Riedmiller, M., 2014. Striving for simplicity: the all convolutional net. In: ICLR (Workshop Track).

Nunes, L.H, Vicente, A.K., 2004. Extreme Precipitation Events in Campinas, brazil. TERRAE Scientific Communications.

Deng, H., Chen, W., Huang, G., 2022. Deep insight into daily runoff forecast- ing based on a cnn-lstm model. Nat. Hazards. https://doi.org/10.1007/s11069-022-05363-2, 10.1007/HYPERLINK.